

# Modeling, Simulation and Optimization of 14nm High-K/Metal Gate NMOS with Taguchi Method

S.K.Mah

*Department of Electrical Engineering  
Faculty of Engineering and Technology  
71800 Nilai, Negeri Sembilan, Malaysia  
mahsiewkien@gmail.com*

I.Ahmad, P.J. Ker, K.P. Tan, Noor Faizah Z. A.

*Institute of Power Engineering  
College of Engineering  
Universiti Tenaga Nasional  
43000 Kajang, Selangor, Malaysia  
Albrahim@uniten.edu.my*

**Abstract**— The developments in electronics technology push the invention of Metal Oxide Semiconductor Field Effect Transistor (MOSFET) towards smaller physical dimension with improvements in both quality and performance. In this paper, design, fabrication and simulation of electrical characteristics of 14nm  $\text{La}_2\text{O}_3/\text{WSi}_2$  NMOS is presented. The fabrication and simulation process of device were performed by using Virtual Wafer Fabrication (VWF) Silvaco TCAD Tools, which consists of ATHENA and ATLAS. The designed device was optimized using Taguchi Method that involves orthogonal arrays and analysis of variance (ANOVA). The original results before optimization process for  $V_{\text{TH}}$  is 0.212648V (7.5% lower than the targeted value) and  $I_{\text{OFF}}$  is  $3.73851 \times 10^{-9}$  A/ $\mu\text{m}$  while the optimized results for  $V_{\text{TH}}$  is 0.233321 V (1.44 % higher than the targeted value) and  $I_{\text{OFF}}$  is  $4.732375 \times 10^{-11}$  A/ $\mu\text{m}$  which fulfilled the targets based on International Technology Roadmap for Semiconductors (ITRS) 2013. The Taguchi optimization method yields a significantly lower  $I_{\text{OFF}}$  with an improved  $I_{\text{ON}}/I_{\text{OFF}}$  ratio by a factor of 25.

**Keywords**—MOSFET, Taguchi, ATHENA, ATLAS

## I. INTRODUCTION

In current fast paced technological era, the development of Si-based ultra large scale integrated circuits (ULSIs) have grown sharply for the last 40 years. The advancement of digitization and Internet of Things (IoT) will further increase the demand for semiconductors such as in smartphones, wearable electronics and IoT devices. The advancements in computer and software technologies have driven the invention of decreasing physical dimension, faster processing speed and reduce power consumption MOSFETs [1]. Thus, technological advancements on Si-ULSIs have provided tremendous computing power in ever device dimensions. Moreover, civilization is very much affected by nanotechnology and much of advancement of nanotechnology is embedded in conventional products of everyday life.

The increasing number of transistor count on ULSIs in the electronic devices has prompted the continued physical feature size scaling of MOSFETs by researchers. MOSFET in smaller physical dimension have higher efficiency, faster switching times, and lower production cost. The size of the

MOSFET has to be scaled down to nanometer regime in order to compete in this challenging microelectronics industry while maintaining excellent functionality and quality.

Through scaling down the physical dimensions of MOSFET, the switching frequency increased with higher transistor drive current. Besides that, higher integration density could be achieved. However, negative effects such as Drain Induced Barrier Lowering (DIBL), and Hot Carrier Effect can affect performance and reliability [2]. All these effects will have impact on the leakage current ( $I_{\text{OFF}}$ ) and will result in increased power consumption. Furthermore, the phenomenon of Short Channel Effect (SCE) occurs when the transistor device reaches nanometer regime. The charge distribution will be influenced due to the changes in electric field at the drain and source area. The SCE is attributed to the electron drift characteristics in the channel which results in modification of the threshold voltage ( $V_{\text{TH}}$ ) [3].

High-k dielectric materials are being introduced as one of the control methods for gate oxide to resolve the problem of excess  $I_{\text{OFF}}$ . Furthermore, higher gate capacitance can be obtained at greater thickness by using high-k dielectric. Considerations on dielectric constant, large band gap and high band offset to silicon, stability, interface quality, process compatibility and reliability should be taken care of, when deciding for an alternative high-k dielectric material. Moreover, the selection of metal gate material with the considerations of matching work function and process integration paired with high-k dielectric material is critical for better performance [4].

In this paper,  $\text{WSi}_2$  has been chosen as the metal gate material and paired with  $\text{La}_2\text{O}_3$  dielectric in a NMOS due to its high thermal stability, high conductivity and high work function [4].  $\text{La}_2\text{O}_3$  gate dielectric has relative high permittivity and large band gap. Thus, it is able to reduce  $I_{\text{OFF}}$  and also enable the further scaling of gate oxide [5]. However, the use of high-k dielectric is quite challenging and difficult due to several issues such as interface control, unsuitable charge trapping causes  $V_{\text{TH}}$  instability, limiting scaling potential below 2 nm, thermal instability, significant mobility degradation and an unclear integration path [6].

Taguchi experimental design is used in this research as statistical optimization method with the aim of identifying controllable factors which give significant impacts on the performance of NMOS. Orthogonal arrays (OAs) design is the statistical method proposed by Dr. Genichi Taguchi [7] to study the parameters with the least number of experiments. The fabrication process of NMOS transistor with the selected high-k material and metal gate was carried out virtually using ATHENA module while the device's electrical characteristics were characterized through ATLAS module [4]. Both modules are obtainable from the SILVACO TCAD simulator. The  $V_{TH}$  and  $I_{OFF}$  are the target values of the critical design characteristics that must be achieved.

## II. PROCESS AND DEVICE STRUCTURE

### A. Fabrication Process

The device was fabricated using ATHENA module. All the fabrication processes were based on similar research on the technology of High-K/Metal Gate [2]. However, design parameters were different since the doping concentrations were optimized according to the specifications of high-k dielectric material and metal gate that were used [8]. The design parameters of 14 nm NMOS is shown in Table I.

TABLE I. FABRICATION RECIPE OF NMOS

Process Step	Parameters
Silicon substrate	<100> orientation
Retrograde well implantation	200Å oxide layer by 970 °C, 20 min of dry oxygen.
	$3.75 \times 10^{12}$ atom/cm <sup>2</sup>
	30 min, 900°C diffused in nitrogen
STI isolation	130Å stress buffer by 900°C, 25 min of dry oxygen
Gate oxide	diffused dry oxygen for 0.1 min, 815°C
$V_{TH}$ adjust implant	$2.7 \times 10^{12}$ atom/cm <sup>2</sup> Boron difluoride
	5keV implant energy, 7° tilt
	20 min annealing at 800 °C
High-K/Metal gate deposition	0.001um La <sub>2</sub> O <sub>3</sub>
	0.038um WSi <sub>2</sub>
	30 min, 800°C annealing
Halo implantation	$6.75 \times 10^{13}$ atom/cm <sup>2</sup> Indium, 30° tilt
Sidewall spacer deposition	0.047um SiN
S/D implantation	$0.98 \times 10^{14}$ atom/cm <sup>2</sup> Arsenic
	12KeV energy dopant, 7° tilt
PMD deposition	20 min, 852°C annealing
Compensation implantation	$0.60 \times 10^{14}$ atom/cm <sup>2</sup> phosphor
	60KeV energy dopant, 7° tilt
Metal 1	0.04 um Aluminum
IMD deposition	0.05 um BPSG
	15 min, 950°C annealing
Metal 2	0.12 um Aluminum

After going through various processing steps in device fabrication, the cross section of the NMOS is depicted in Fig. 1. The NMOS has metal layer, oxide layer and semiconductor layer.

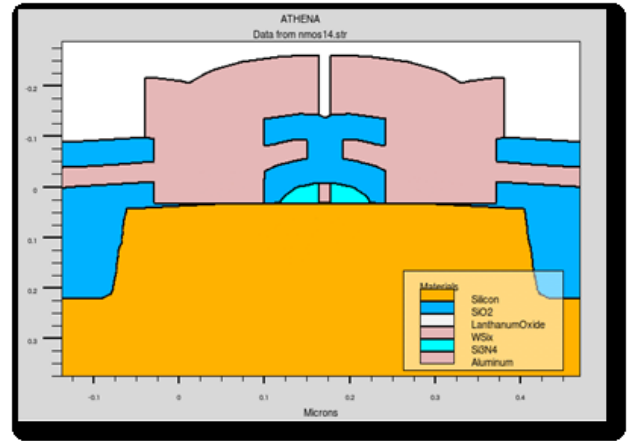


Fig. 1. Cross section of NMOS.

### B. Taguchi L9 (3<sup>4</sup>) Orthogonal Array Method

After the designed NMOS has been successfully fabricated and simulated, process parameters were optimized through Taguchi method by using experimental layout of L9 OA [9]. The values of the different levels of control factors are shown in Table II. Two noise factors (NF) were evaluated in the experiments as shown in Table III.

TABLE II. CONTROL FACTORS AND THEIR LEVELS

Control Factor	Unit	Level 1	Level 2	Level 3
Halo Implantation	atom/cm <sup>2</sup>	$6.65 \times 10^{13}$	$6.75 \times 10^{13}$	$6.80 \times 10^{13}$
Halo Tilt Angle	°	29	30	31
S/D Implantation	atom/cm <sup>2</sup>	$0.97 \times 10^{14}$	$0.98 \times 10^{14}$	$1.00 \times 10^{14}$
Compensation Implantation	atom/cm <sup>2</sup>	$0.59 \times 10^{14}$	$0.60 \times 10^{14}$	$0.61 \times 10^{14}$

TABLE III. NOISE FACTORS AND THEIR LEVELS

Noise Factor (NF)	Unit	Level 1	Level 2
Sacrificial Oxide Layer Temperature	°C	910 (N1)	915 (N2)
Annealing Temperature	°C	950 (M1)	949 (M2)

## III. RESULTS AND DISCUSSION

### A. Simulation of Electrical Characteristics

The designed NMOS was simulated in Silvaco TCAD in the ATLAS module. The simulation results for electrical characteristics of the NMOS are shown in Fig. 2 and Fig. 3.

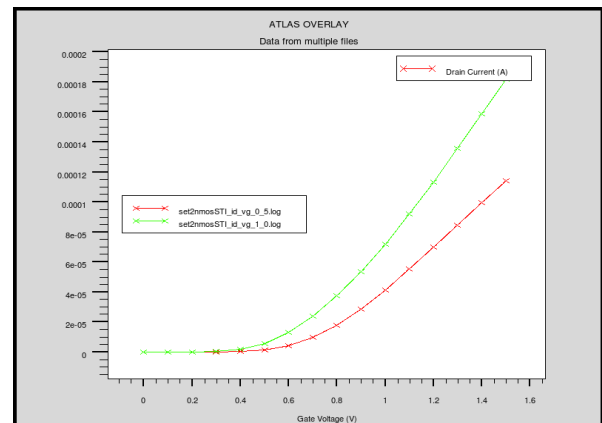
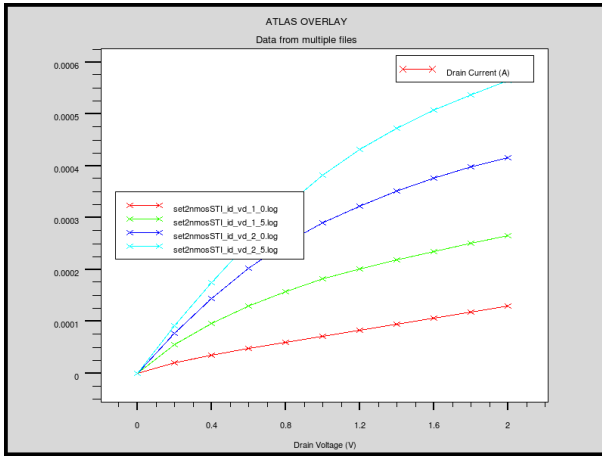


Fig. 2.  $I_D - V_{GS}$  Curve


 Fig. 3.  $I_D - V_{DS}$  Curve

### B. Optimization using Taguchi L9

Nine sets of different experiments for NMOS with 4 noise factors N1, N2, M1 and M2 were simulated according to the process parameter combinations as specified in the L9 OA. The simulation results for  $V_{TH}$  and  $I_{OFF}$  are shown in Table IV and Table V respectively.

 TABLE IV. RESULTS OF  $V_{TH}$  (V)

Exp. No	Threshold Voltage ( $V_{TH}$ )			
	N1M1	N1M2	N2M1	N2M2
1	0.287137	0.323786	0.287239	0.323885
2	0.0824418	0.120627	0.0825364	0.12072
3	-0.1388	-0.10289	-0.138714	-0.10281
4	0.122842	0.158831	0.122936	0.158924
5	0.291788	0.329504	0.291888	0.329601
6	0.197709	0.237258	0.197802	0.237361
7	0.263194	0.303888	0.263295	0.303987
8	0.176829	0.212477	0.176922	0.212569
9	0.375447	0.412502	0.375544	0.412596

 TABLE V. RESULTS OF  $I_{OFF}$  (A/ $\mu$ m)

Exp No	Threshold Voltage ( $V_{TH}$ )			
	N1M1	N1M2	N2M1	N2M2
1	$1.29416 \times 10^{-9}$	$7.83379 \times 10^{-10}$	$1.29224 \times 10^{-9}$	$7.82228 \times 10^{-10}$
2	$2.88000 \times 10^{-8}$	$1.63584 \times 10^{-8}$	$2.87581 \times 10^{-8}$	$1.63347 \times 10^{-8}$
3	$8.07082 \times 10^{-7}$	$4.89497 \times 10^{-7}$	$8.06113 \times 10^{-7}$	$4.88885 \times 10^{-7}$
4	$1.54360 \times 10^{-8}$	$9.04752 \times 10^{-9}$	$1.54135 \times 10^{-8}$	$9.03434 \times 10^{-9}$
5	$1.22881 \times 10^{-9}$	$7.3029 \times 10^{-10}$	$1.22701 \times 10^{-9}$	$7.29227 \times 10^{-10}$
6	$4.63438 \times 10^{-9}$	$2.64795 \times 10^{-9}$	$4.62573 \times 10^{-9}$	$2.64406 \times 10^{-9}$
7	$1.87076 \times 10^{-9}$	$1.07614 \times 10^{-9}$	$1.86802 \times 10^{-9}$	$1.07458 \times 10^{-9}$
8	$6.48804 \times 10^{-9}$	$3.80172 \times 10^{-9}$	$6.47847 \times 10^{-9}$	$3.79616 \times 10^{-9}$
9	$3.41084 \times 10^{-10}$	$2.00191 \times 10^{-10}$	$3.40583 \times 10^{-10}$	$1.99899 \times 10^{-10}$

Next was the process of finding the appropriate control factor levels to make the process less sensitive to variations in noise by studying the response variation using signal-to-noise (S/N) ratio. The optimal combinations were determined through signal-to-noise (S/N) ratio [4]. The level with the highest S/N ratio for each control factor was selected as to achieve better quality characteristic [10].

The quality characteristics in S/N ratio analysis are categorized into smaller-the-better (STB), larger-the-better (LTB) and nominal-the-best (NTB) performance characteristics [11].  $V_{TH}$  analysis was determined by NTB characteristic while  $I_{OFF}$  analysis was determined by STB

characteristic [12]. The S/N ratio for  $V_{TH}$  and  $I_{OFF}$  are shown in Table VI and Table VII respectively.

 TABLE VI. S/N RATIO OF PROCESS PARAMETERS FOR  $V_{TH}$ 

Symbol	Process Parameter	S/N Ratio (Nominal-the-Best)			Total Mean S/N
		Level 1	Level 2	Level 3	
A	Halo Implantation	17.26	19.76	22.15	19.72
B	Halo Tilt Angle	20.48	18.63	20.06	
C	S/D Implantation	20.76	18.40	20.01	
D	Compensation Implantation	23.86	18.16	17.15	

 TABLE VII. S/N RATIO OF PROCESS PARAMETERS  $I_{OFF}$ 

Symbol	Process Parameter	S/N Ratio (Smaller-the-Better)			Total Mean S/N
		Level 1	Level 2	Level 3	
A	Halo Implantation	151.86	168.78	177.63	166.09
B	Halo Tilt Angle	171.25	166.00	161.02	
C	S/D Implantation	171.13	167.22	159.92	
D	Compensation Implantation	183.47	165.80	148.99	

### C. Analysis of Variance (ANOVA)

Analysis of variance (ANOVA) is a collection of statistical techniques used to analyze the percentage contribution of each individual control factor on the entire process [9]. Thus, ANOVA was used to determine the ranking of impact of the control factors towards  $V_{TH}$  and  $I_{OFF}$ . The ANOVA results for  $V_{TH}$  and  $I_{OFF}$  are tabulated Table VIII and Table IX respectively. The higher percentage on factor effect indicates the particular control factor contributes larger effect to the NMOS in terms of  $V_{TH}$  and  $I_{OFF}$ .

 TABLE VIII. ANOVA ANALYSIS FOR  $V_{TH}$ 

Symbol	Process Parameter	Factor Effect	
		NTB	Mean
A	Halo Implantation	28	28.99
B	Halo Tilt Angle	4	2.40
C	S/D Implantation	7	3.53
D	Compensation Implantation	61	29.57

 TABLE IX. ANOVA ANALYSIS FOR  $I_{OFF}$ 

Symbol	Process Parameter	Factor Effect
		STB
A	Halo Implantation	33
B	Halo Tilt Angle	5
C	S/D Implantation	6
D	Compensation Implantation	56

According to Table VIII, Compensation Implantation (D) has the most dominant factor effect while Halo Implantation (A) was identified as the adjustment factor, while Halo Tilt Angle (B) and S/D Implantation (C) acted as pooled factors for  $V_{TH}$ . For  $I_{OFF}$ , ANOVA was used to find the highest factor effect contribution by a control factor, namely the dominant factor for  $I_{OFF}$ . Thus, Compensation Implant (D) which has the highest factor effect was defined as the dominant factor as shown in Table IX.

#### D. Confirmation Test

Confirmation tests for both  $V_{TH}$  and  $I_{OFF}$  were carried out in the final phase of this work. The objective of the confirmation test is to verify the final results after optimization using Taguchi method [9]. The best setting for  $V_{TH}$  was defined as A1B2C2D1 while for  $I_{OFF}$ , it was A3B1C1D1. Table X shows the best setting of process parameters for confirmation runs performed for  $V_{TH}$  and  $I_{OFF}$ . Table XI and Table XII show the final results of confirmation test for  $V_{TH}$  and  $I_{OFF}$ .

TABLE X. BEST SETTING OF PROCESS PARAMETERS

Symbol	Process Parameter	Unit	Best Value	
			$V_{TH}$	$I_{OFF}$
A	Halo Implantation	atom/cm <sup>2</sup>	6.65x10 <sup>13</sup>	6.80x10 <sup>13</sup>
B	Halo Tilt Angle	°	30	29
C	S/D Implantation	atom/cm <sup>2</sup>	0.98x10 <sup>14</sup>	0.97x10 <sup>14</sup>
D	Compensation Implantation	atom/cm <sup>2</sup>	0.59x10 <sup>14</sup>	0.59x10 <sup>14</sup>

TABLE XI. CONFIRMATION TEST RESULT OF  $V_{TH}$  (V)

Noise Factor (N & M)				Best Value	
<i>NIM1</i>	<i>NIM2</i>	<i>N2M1</i>	<i>N2M2</i>	<i>NTB</i>	<i>Mean</i>
0.212935	0.253605	0.213038	0.253706	19.94	-12.64

According to ANOVA analysis and S/N ratio, the predicted S/N ratio for NTB falls between 14.27 dB to 22.01 dB. While the predicted S/N ratio for mean falls between -11.70 dB to -19.44 dB. This clearly shows that the obtained S/N ratio for NTB (19.94 dB) and mean (-12.64 dB) after optimization are in very good agreement with experimental. Furthermore, the average value of  $V_{TH}$  after optimization is 0.233321V (1.44 % higher than the targeted value).

TABLE XII. CONFIRMATION TEST RESULT OF  $I_{OFF}$  (A/ $\mu$ m)

Noise Factor (N & M)				Best Value	
<i>NIM1</i>	<i>NIM2</i>	<i>N2M1</i>	<i>N2M2</i>	<i>STB</i>	
5.84952 ×10 <sup>-11</sup>	3.62233 ×10 <sup>-11</sup>	5.84065 ×10 <sup>-11</sup>	3.617 ×10 <sup>-11</sup>	206.5	

According to Taguchi method, the predicted S/N ratio for STB falls between 179.78 dB to 220.34 dB. This shows that the obtained S/N ratio for  $I_{OFF}$  (206.5 dB) after optimization is within the predicted range. Besides, the average value of  $I_{OFF}$  after optimization is 4.732375x10<sup>-11</sup> A/ $\mu$ m.

Through optimization process, the original result has been optimized from 0.212648 V (7.5% lower than the targeted value) to 0.233321 V (1.44 % higher than the targeted value) for  $V_{TH}$  and  $I_{OFF}$  from 3.73851x10<sup>-9</sup> A/ $\mu$ m to 4.732375x10<sup>-11</sup> A/ $\mu$ m. The average results after optimization for  $V_{TH}$  and  $I_{OFF}$  are shown in Table XIII and are compared with ITRS 2013 prediction.

TABLE XIII. AVERAGE RESULT OF CONFIRMATION TEST

Controlled Parameter	ITRS 2013 Prediction	Average Result
$V_{TH}$ (V)	0.230±12.7%	0.233321 (+1.44%)
$I_{OFF}$ (A/ $\mu$ m)	100 x10 <sup>-9</sup>	4.732375x10 <sup>-11</sup>

#### IV. CONCLUSION

This work has fulfilled the objectives and the simulation results have proven the possibility of fabricating 14nm La<sub>2</sub>O<sub>3</sub>/WSi<sub>2</sub> NMOS. Original results for the designed NMOS are 0.212648V for  $V_{TH}$  and 3.73851x10<sup>-9</sup>A/ $\mu$ m for  $I_{OFF}$ . Then, Taguchi optimization was performed to optimize the process factors. The results obtained are compared with the predicted values of S/N ratio and ANOVA analysis. By using Taguchi method, the average  $V_{TH}$  of 0.233321V was observed with the control factors of A1B2C2D1. For  $I_{OFF}$ , the average value of 4.732375x10<sup>-11</sup>A/ $\mu$ m was obtained. Therefore, this work has successfully demonstrated that La<sub>2</sub>O<sub>3</sub>/WSi<sub>2</sub> NMOS can be fabricated and optimized with both  $V_{TH}$  and  $I_{OFF}$  values fall within ITRS 2013 prediction.

#### ACKNOWLEDGMENT

The authors gratefully acknowledge the Tenaga Nasional Berhad (TNB) Seeding fund (Project code: U-TG-RD-18-04) for the access to the simulation software.

#### REFERENCES

- [1] N. B. Atan, I. B. Ahmad, and B. B. Y. Majlis, "Effects of high-K dielectrics with metal gate for electrical characteristics of 18nm NMOS device," in 2014 IEEE International Conference on Semiconductor Electronics (ICSE2014), 2014, pp. 56-59.
- [2] Z. A. N. Faizah, I. Ahmad, P. J. Ker, P. S. A. Roslan, and A. H. A. Maharan, "Modeling of 14 nm gate length n-Type MOSFET," in 2015 IEEE Regional Symposium on Micro and Nanoelectronics (RSM), 2015, pp. 1-4.
- [3] A. H. A. Maharan, P. S. Menon, I. Ahmad, H. A. Elgomati, B. Y. Majlis, and F. Salehuddin, "Scaling down of the 32 nm to 22 nm gate length NMOS transistor," in 2012 10th IEEE International Conference on Semiconductor Electronics (ICSE), 2012, pp. 173-176.
- [4] N. F. Zainul Abidin, "Statistical Modeling for 32 nm High-k Metal Gate Technology of Silicon MOSFET Device," Master, College of Engineering, Universiti Tenaga Nasional, Kajang, Malaysia, 2014.
- [5] T. Koyanagi, K. Tachi, K. Okamoto, K. Kakushima, P. Ahmet, K. Tsutsui, et al., "Electrical characterization of La<sub>2</sub>O<sub>3</sub>-gated metal oxide semiconductor field effect transistor with Mg incorporation," Japanese Journal of Applied Physics, vol. 48, p. 05DC02, 2009.
- [6] S.-H. Lo, D. Buchanan, Y. Taur, and W. Wang, "Quantum-mechanical modeling of electron tunneling current from the inversion layer of ultra-thin-oxide nMOSFETs," IEEE Electron Device Letters, vol. 18, pp. 209-211, 1997.
- [7] K.-L. Tsui, "An overview of Taguchi method and newly developed statistical methods for robust design," IIE Transactions, vol. 24, pp. 44-57, 1992.
- [8] S.K. Mah, I. Ahmad, P.J. Ker, Noor Faizah Z.A., "Modelling of 14NM Gate Length La<sub>2</sub>O<sub>3</sub> -based n-Type MOSFET," Journal of Telecommunication, Electronic and Computer Engineering, pp. 107-110, 2016.
- [9] H. Ramakrishnan, S. Shedabale, G. Russell, and A. Yakovlev, "Analysing the effect of process variation to reduce parametric yield loss," in Integrated Circuit Design and Technology and Tutorial, 2008. ICICDT 2008. IEEE International Conference on, 2008, pp. 171-176.
- [10] N. Naidu, "Mathematical model for quality cost optimization," Robotics and Computer-Integrated Manufacturing, vol. 24, pp. 811-815, 2008.
- [11] P. J. Ross, Taguchi Techniques for Quality Engineering: Loss Function, Orthogonal Experiments, Parameter and Tolerance Design., 2nd Edition ed.: McGraw-Hill, New York, 1996.
- [12] S. Fauziyah, I. Ahmad, F. Azlee Hamid, A. Zaharim, H. Elgomati, B. Yeop Majlis, et al., "Optimization of HALO structure effects in 45nm p-type MOSFETs device using Taguchi Method," International Journal of Engineering and Applied Sciences, pp. 80-86, 2011.